

# Modeling Thermo-Mechanical Stress of Flexible CIGS Solar Cells

Hansung Kim , Member, IEEE, Da Xu, Ciby John, and Yaqiong Wu

**Abstract**—Copper indium gallium diselenide (CIGS) thin-film solar cells are fabricated through several deposition and annealing processes at high temperatures, which can generate significant thermal residual stress to solar cells. Moreover, since CIGS solar cells with flexible substrates are rollable and bendable, they are susceptible to mechanical stresses during these processes. In addition, partial shading (hotspot) can exert high heat on the CIGS solar cell. In this paper, we investigate the thermo-mechanical stress of each active layer of CIGS solar cells due to annealing, external bending, and hotspot using finite element method (FEM). We found that average stress of each active layer decreases and maximum stress in the cell increases when interface crack is introduced between cadmium sulfide (CdS)/CIGS. Our overarching goal is to quantify the relationship between the fabrication/operating process and the reliability of CIGS solar cells (energy release rate and internal stresses), which could improve the reliability of flexible solar cells. It is also found that lowering the annealing temperature can reduce the stresses in the cells and lowering CIGS thickness can reduce the delamination probability of CdS/CIGS interface. Finally, we investigate the effect of the crack length of the CdS/CIGS interface on the electrical performance of CIGS solar cells through FEM simulations. We found that as the crack size between CdS and CIGS layers increases, short-circuit current density decreases, while open-circuit voltage remains almost constant.

**Index Terms**—Copper indium gallium diselenide (CIGS) thin-film solar cells, finite element method (FEM), reliability.

## I. INTRODUCTION

**R**ELIABILITY of thin-film solar cells should be thoroughly investigated in order to develop robust thin-film solar cells. Nowadays, flexible solar cells are used for clothing, to charge small electronics, and as roofing material to generate electricity for residential use. Copper indium gallium diselenide (CIGS) solar cells are one of the most prominent thin-film flexible solar cells on the market. Typical active layers of CIGS solar cells are zinc oxide (ZnO), cadmium sulfide (CdS), and

CIGS. Common fabrication methods for each layer of CIGS solar cells are as follows:

- 1) co-evaporation for the CIGS layer (400–550 °C);
- 2) chemical bath deposition for the CdS layer (60–90 °C);
- 3) sputtering for the ZnO layer (room temperature).

In some cases, high-temperature annealing treatment is carried out to improve the efficiency of solar cells by improving the crystalline quality of active layers. The temperature range of the annealing process is between 200 and 450 °C. However, there is a possibility of generating cracks or porous holes at the layer interfaces during or after the annealing process [1], [2]. Bremaud [1] reported the emergence of a small crack near the interface between the CIGS and CdS layers. He also reported small holes in several grains in the CIGS layer. Park *et al.* [2] reported the emergence of continuous porous holes at the interface between CdS and CIGS during the annealing process above 200 °C. These porous holes can act as a “stress riser,” like a small crack when thermo-mechanical loads are applied to the solar cell. However, they did not observe any holes or cracks at the ZnO/CdS interface region.

Even though thin-film solar cells are bendable and rollable, excessive external loading during operation could generate significant internal stress resulting in some cracks and even delamination of interface layers. Lee *et al.* [3] investigated the critical strain above which flexible PbS/CdS thin-film solar cells start decreasing in efficiency. They reported that PbS/CdS thin-film solar cells start producing surface channel cracks at 1.1% strain and also begin to decrease the efficiency. They reported that short-circuit current density ( $J_{sc}$ ) significantly decreases as the applied strain increases after 1.1% strain is applied, while open-circuit voltage ( $V_{oc}$ ) is minimally influenced. Generally, 1% strain limit is considered the design parameter for flexible electronic devices [4]. Mei *et al.* [5] and Chai and Fox [6] reported interfacial delamination of multilayered thin films when significant external loadings are applied to the thin films.

Abrupt temperature increase due to a hotspot is another critical issue for the reliability of CIGS solar cells. When solar cells are partially shaded, those shaded regions can induce reverse-bias conditions, generating a significant temperature increase, which is called hotspot. Lee *et al.* [7] reported the formation of voids at the heterogeneous interfaces in the CIGS solar cells caused by hotspot. Nardone *et al.* [8] simulated the temperature distribution of a CIGS solar cell with 20% shading. He presented that the CIGS cell can reach up to 425 °C after 600 s of hotspot exposure. One method of protecting a solar cell from hotspot damage is to use the bypass diode. However, it is reported by

Manuscript received October 5, 2018; revised December 21, 2018; accepted January 8, 2019. Date of publication January 31, 2019; date of current version February 18, 2019. This work was supported in part by Purdue PRF Faculty Research Grant and in part by the Grants provided by the College of Engineering and Science Purdue University Northwest. (Corresponding author: Hansung Kim.)

The authors are with the Department of Mechanical and Civil Engineering, Purdue University Northwest, Hammond, IN 46323-2094 USA. (e-mail: kim886@purdue.edu; dax@pnw.edu; john6@pnw.edu; wu958@pnw.edu).

Color versions of one or more of the figures in this paper are available online at <http://ieeexplore.ieee.org>.

Digital Object Identifier 10.1109/JPHOTOV.2019.2892531

several researchers that the bypass diode is not always sufficient to prevent hotspot damage in thin-film solar cells [7], [9]. So, high temperatures induced by hotspots can generate significant internal stresses in a solar cell possibly contributing the layer delamination of thin-film solar cells.

In this research, we will address the following questions to examine the reliability of CIGS solar cells.

- 1) What are the effects of initial crack, annealing temperature, bending load, and hotspot temperature on the thermo-mechanical stresses of the cell? How can we quantify them?
- 2) What is the effect of layer thickness on the probability of layer delamination? How can we quantify the effect?

To answer the above questions, we investigated thermo-mechanical stress of each active layer and energy release rate of CIGS solar cells due to annealing, external bending, and hotspot using finite element method (FEM). For the above simulations, we used two scenarios: the first with a  $1 \mu\text{m}$  initial crack, and the second without any initial crack. We investigated the effect of the crack only for the CdS/CIGS interface because most of the published literatures reported the appearance of crack or porous holes at the CdS/CIGS interface after annealing. First, we simulated the residual stress on a CIGS solar cell caused by cooling to room temperature from annealing temperatures of 200, 300, and 400 °C, in order to quantify the relationship between the annealing temperature and internal stresses of the CIGS solar cell. Second, we examined the internal stresses of active layers of the CIGS solar cell after applying external bending loads of 1%, 1.5%, and 2% maximum strain to examine the relationship between the bending load and internal stresses of the CIGS cell. Furthermore, we increase the bending load up to 5% strain to investigate an extreme case. Third, we applied hotspot temperatures of 200, 300, and 400 °C to the CIGS cell, which already had the initial stress due to annealing and bending. We investigated the internal stress of each active layer after cooling down to room temperature from the above hotspot temperatures to quantify the relation between hotspot temperature and internal stresses caused by hotspot. We calculated the energy release rate of CIGS cells with an initial crack to examine how annealing, bending, and hotspot contribute to the layer delamination of the CIGS/CdS interface. Moreover, we changed the thickness of each layer to investigate the effect of layer thickness on layer delamination: ZnO (200–600 nm), CdS (50–70 nm), and CIGS (1–3  $\mu\text{m}$ ). Finally, we investigated the effect of delamination length at the CdS/CIGS interface on the electrical performance of CIGS solar cells.

## II. METHOD

### A. Simulation Procedure

We used COMSOL Multiphysics software for our FEM simulation since it can solve heat transfer, solid mechanics, and semiconductor simulations in the same framework. The thermo-mechanical properties of CIGS active layers are illustrated in Table I. The active layers are assumed to be linear elastic materials. The parameters were obtained from published literature [1], [10]–[12]. However, if published values are described as a range of values, we used an average value of the range.

TABLE I  
THERMO-MECHANICAL PROPERTIES OF ACTIVE LAYERS

	CIGS	CdS	ZnO
Young's modulus (GPa)	78.5 (average) [10]	46 [11]	173 [12]
Poisson's ratio	0.35 (average) [10]	0.344 [11]	0.33 [12]
Density ( $\text{g}/\text{cm}^3$ )	5.9 [1]	4.8 [1]	5.6 [1]
Thermal expansion coefficient ( $10^{-6} \text{K}^{-1}$ )	9.5 (average) [1]	4.5 [1]	3.8 (average) [1]

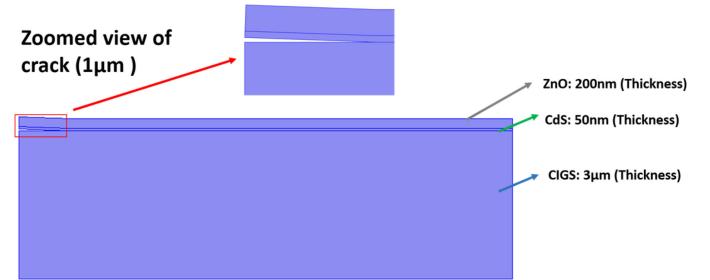


Fig. 1. CIGS solar cells with  $1 \mu\text{m}$  initial crack.

Fig. 1 shows the 2-D schematics of CIGS solar cells ( $10 \times 3.25 \mu\text{m}$ ) with a  $1 \mu\text{m}$  initial crack at the interface between CdS and CIGS. The thickness of each layer is based on Gloeckler *et al.*'s baseline model [13]. The initial crack is generated by separating the CdS layer from the CIGS layer geometrically. However, parametric study of the effect of crack length, location, and angle on thermo-mechanical stress of CIGS cell is not carried out in this study, which could be future work of our group. For thermo-mechanical stress analysis of CIGS solar cells, we performed FEM simulation with a 2-D plane strain assumption.

When the energy release rate of an interface crack tip is larger than a critical energy release rate, the interface delamination takes place. For linear elastic materials, the energy release rate can be calculated by  $J$ -integral [14], which is a 2-D line integral following a counterclockwise contour,  $\Gamma$ , enclosing the crack tip.  $J$ -integral is calculated based on the following equation:

$$J = \int \left( W n_x - T_i \frac{\partial u_i}{\partial x} \right) ds$$

where  $W$  is the strain energy density described as follows:

$$W = \frac{1}{2} (\sigma_x \varepsilon_x + \sigma_y \varepsilon_y + \sigma_{xy} 2\varepsilon_{xy}).$$

$T$  is the traction vector defined as follows:

$$T = [\sigma_x n_x + \sigma_{xy} n_y, \sigma_{xy} n_x + \sigma_y n_y].$$

$\sigma_{ij}$  is the stress component,  $\varepsilon_{ij}$  is the strain component, and  $n_i$  is the normal vector component.

Mesh size of crack tip and interface is  $\sim 0.01 \mu\text{m}$ , while that of active layers gradually increases when moving away from the interface. The largest mesh size is  $\sim 0.5 \mu\text{m}$  for the CIGS layer,  $\sim 0.02 \mu\text{m}$  for the CdS layer, and  $\sim 0.05 \mu\text{m}$  for the ZnO layer.

Moreover, thermal stress due to temperature change is calculated based on the following equation:

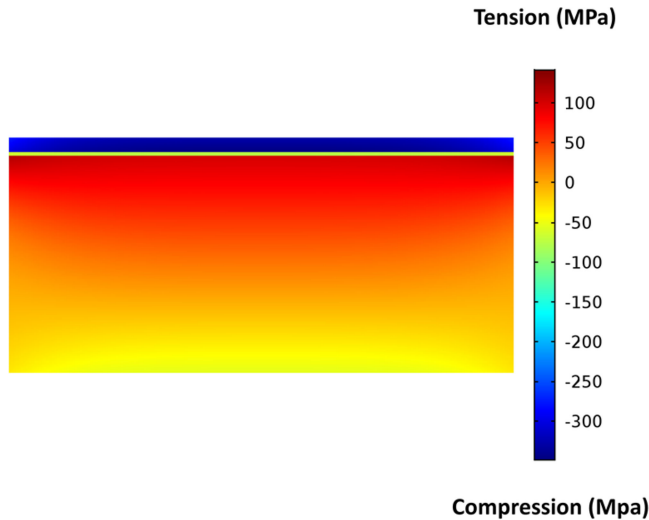


Fig. 2. Stress of CIGS cell after cooling down to room temperature from annealing at 400 °C.

TABLE II  
STRESSES OF CIGS CELL AFTER COOLING DOWN TO ROOM TEMPERATURE FROM ANNEALING AT 400 °C

	Stress without crack (MPa)	Stress with crack (MPa)
ZnO layer (Avg)	-281 (C)	-257 (C)
CdS layer (Avg)	-66 (C)	-59 (C)
CIGS layer (Avg)	20 (T)	18 (T)
Maximum stress for T	147 (T)	730 (T)
Maximum stress for C	-348 (C)	-1063 (C)

C: Compression, T: Tension.

$\sigma_{th} = E\varepsilon_{th}$ , where  $\sigma_{th}$ : Thermal stress,  $E$ : Young's modulus,  $\varepsilon_{th}$ : Thermal strain

$\varepsilon_{th} = \alpha(T-T_{ref})$ , where  $\alpha$ : Thermal expansion coefficient,  $T$ : Temperature.

For current–voltage ( $I$ – $V$ ) simulation of CIGS solar cells, we used electrical parameters and a generation rate of each active layer based on Gloeckler *et al.*'s baseline model [13], [15]. In order to investigate the effect of delamination length of CdS/CIGS interface on the electrical performance, we generated delamination lengths of 2, 4, 6, and 8  $\mu\text{m}$  by separating the CdS layer from the CIGS layer, which corresponds to 20%, 40%, 60%, and 80% delamination since the total length of our CIGS cell is 10  $\mu\text{m}$ . A more detailed procedure of electrical performance simulation can be found in our previous paper [16].

### III. RESULTS AND DISCUSSION

#### A. Annealing Temperature Effect on Internal Stresses

Fig. 2 illustrates the thermal stress of the CIGS solar cell after cooling down to room temperature from annealing at 400 °C. As shown in Table II, regardless of the existence of an initial crack, most of the ZnO and CdS layers are in compression, while the

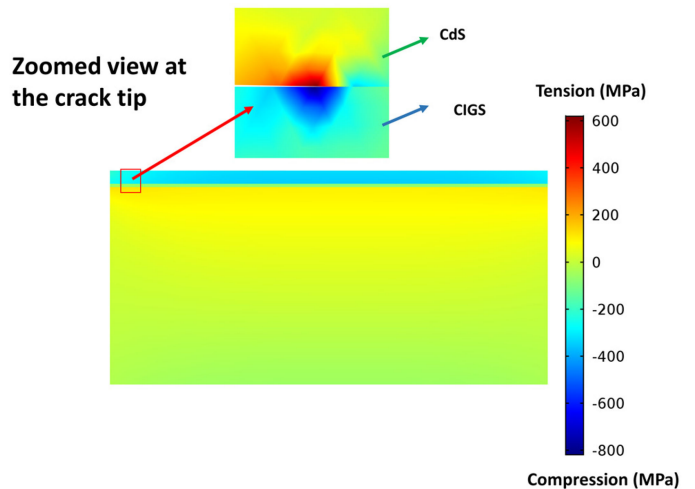


Fig. 3. Thermal stress of CIGS cell after cooling down to room temperature from annealing of CIGS solar cells with 1  $\mu\text{m}$  crack at 400 °C.

TABLE III  
STRESSES OF CIGS CELL WITHOUT CRACK AFTER COOLING DOWN TO ROOM TEMPERATURE FROM VARIOUS ANNEALING TEMPERATURES

Annealing temperature	200 °C	300 °C	400 °C
ZnO layer stress (Avg)	-133 (C)	-207 (C)	-281 (C)
CdS layer stress (Avg)	-33 (C)	-49 (C)	-66 (C)
CIGS layer stress (Avg)	9 (T)	15 (T)	20 (T)
Maximum stress for T	70 (T)	109 (T)	147 (T)
Maximum stress for C	-165 (C)	-256 (C)	-348 (C)

Unit of stress in MPa. C: Compression, T: Tension.

average stress of CIGS is in tension. However, if investigated in detail, the upper part of the CIGS layer is in tension, while the lower part of the CIGS layer is in compression. The maximum compressive stress in the CIGS layer for CIGS solar cells without cracks is found to be 55 MPa, which reasonably agrees with experimental values (66–72 MPa) [10]. Fig. 3 illustrates the thermal stress of CIGS solar cells with an initial crack after cooling down to room temperature from annealing at 400 °C. The magnitude of maximum tension and maximum compression stress in the CIGS cell with the initial crack are much larger than those of the CIGS cell without crack as shown Table II. However, the average stresses for the ZnO, CdS, and CIGS layers for the CIGS cell with the crack are smaller than those of the CIGS cell without crack as shown in Table II. Table III describes the stress of each layer and maximum stress in the CIGS cell without cracks after cooling down to room temperature from various annealing temperatures. As shown in Table III, the stress of each layer increases as annealing temperature increases.

Table IV shows the effect of annealing temperature on the stresses and  $J$ -integral of the CIGS cell with an initial crack. Just like the CIGS without the crack, the stress of each layer increases as the annealing temperature increases. Since the  $J$ -integral is increasing with the annealing temperature, the probability of layer delamination increases with higher annealing temperatures.

TABLE IV  
STRESSES AND J-INTEGRAL OF CIGS CELL WITH AN INITIAL CRACK AFTER COOLING DOWN TO ROOM TEMPERATURE FROM VARIOUS ANNEALING TEMPERATURES

Annealing temperature	200 °C	300 °C	400 °C
ZnO layer stress (Avg)	-122 (C)	-190 (C)	-257 (C)
CdS layer stress (Avg)	-28 (C)	-43 (C)	-59 (C)
CIGS layer stress (Avg)	9 (T)	13 (T)	18 (T)
Maximum stress for T	346 (T)	538 (T)	730 (T)
Maximum stress for C	-503 (C)	-783 (C)	-1063 (C)
J-integral (J/m <sup>2</sup> )	0.00097	0.0023	0.0043

Unit of stress in MPa. C: Compression, T: Tension.

TABLE V  
STRESSES OF CIGS CELL WITHOUT A CRACK AFTER APPLYING VARIOUS BENDING DISPLACEMENTS TO THE CIGS CELL WHICH ALREADY HAD RESIDUAL STRESS FROM COOLING DOWN TO ROOM TEMPERATURE FROM 400 °C ANNEALING

bending displacement	0.04 μm	0.08 μm	0.115 μm
ZnO layer stress (Avg)	-538 (C)	-677 (C)	-798 (C)
CdS layer stress (Avg)	-123 (C)	-158 (C)	-188 (C)
CIGS layer stress (Avg)	38 (T)	48 (T)	56 (T)
Maximum stress for T	1584 (T)	1881 (T)	2141 (T)
Maximum stress for C	-1474 (C)	-1634 (C)	-1774 (C)

Unit of stress in MPa. C: Compression, T: Tension.

Based on simulation results, we recommend manufacturers of CIGS solar cells to use the lowest annealing temperature possible in order to reduce thermal stresses in the cell.

### B. Bending Load Effect on Internal Stresses

In order to examine the effect of bending on the internal stresses of CIGS cells, we fixed the right boundary of the CIGS cell and applied the displacement of 0.04, 0.08, and 0.115 μm to the left bottom point, which generated 1%, 1.5%, and 2% maximum strain on the CIGS cells. This bending simulation was carried out on the CIGS cell, which already had residual stress from the previous annealing simulation. Table V shows the simulation results of various bending loads, which confirms that stress increases as the bending load increases.

To verify the simulation results, we compared our simulation results with analytical calculations. In order to calculate the bending stress analytically, first, we identified the forces which can generate each bending displacement. Second, the bending moment caused by each force was calculated along the length of the CIGS cell using method of section [17]. Third, bending stress ( $\sigma$ ) was calculated as shown in the following [17]:

$$\sigma = \frac{My}{I}$$

where  $M$ : Bending moment,  $y$ : distance from centroid (at the cross section),  $I$ : second area moment of inertia of the cross section.

Finally, bending stress is added to the previously obtained residual stress caused by 400 °C annealing. Fig. 4 compares the analytical solution with FEM results for different bending loads

TABLE VI  
STRESSES AND J-INTEGRAL OF CIGS CELL WITH AN INITIAL CRACK AFTER APPLYING VARIOUS BENDING DISPLACEMENTS TO THE CELL WHICH ALREADY HAD RESIDUAL STRESS FROM COOLING DOWN TO ROOM TEMPERATURE FROM 400 °C ANNEALING

bending displacement	0.04 μm	0.08 μm	0.115 μm
ZnO layer stress (Avg)	-515 (C)	-656 (C)	-779 (C)
CdS layer stress (Avg)	-117 (C)	-152 (C)	-182 (C)
CIGS layer stress (Avg)	36 (T)	46 (T)	55 (T)
Maximum stress for T	1251 (T)	1209 (T)	1283 (T)
Maximum stress for C	-1970 (C)	-2132 (C)	-2273 (C)
J-integral (J/m <sup>2</sup> )	0.28	0.33	0.37

Unit of stress in MPa. C: Compression, T: Tension.

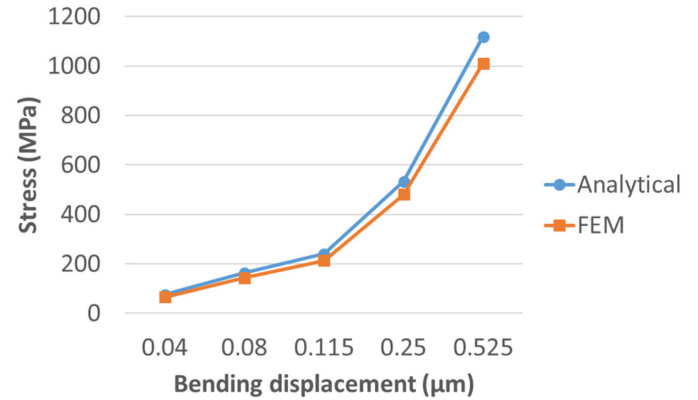


Fig. 4. Comparison of stress for a midpoint along the bottom of CIGS cell for different bending displacements. Bending displacement is applied to the CIGS cell, which already has a residual stress due to 400 °C annealing.

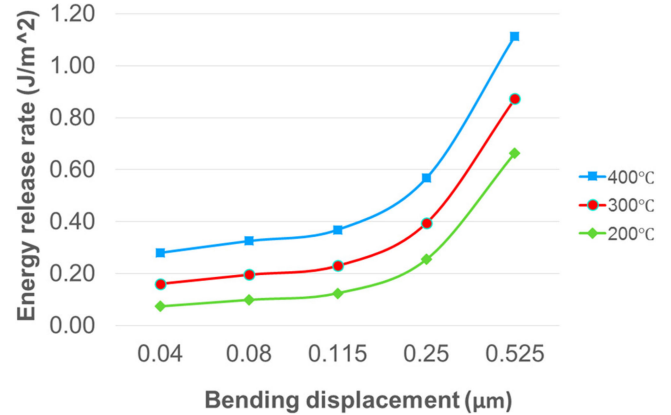


Fig. 5. Energy release rate of a CIGS cell with an initial crack for different bending displacements with different annealing temperatures.

for a midpoint along the bottom of CIGS cell, which shows a strong agreement.

Moreover, Table VI shows the effect of bending displacement on the stresses and  $J$ -integral of CIGS cell with an initial crack after 400 °C annealing. Just like the CIGS cell without crack, the stress of each layer increases as bending displacement increases. Fig. 5 illustrates the energy release rate as a function of bending displacement and annealing temperature. As bending displacement and annealing temperature increase,

TABLE VII  
STRESSES OF CIGS CELL WITHOUT A CRACK AFTER COOLING DOWN TO ROOM TEMPERATURE FROM VARIOUS HOTSPOT TEMPERATURES (USING THE CELL WITH PREVIOUS 400 °C ANNEALING AND 1% MAX BENDING)

Hotspot temperature	200 °C	300 °C	400 °C
ZnO layer stress (Avg)	-415 (C)	-489 (C)	-563 (C)
CdS layer stress (Avg)	-97 (C)	-115 (C)	-132 (C)
CIGS layer stress (Avg)	29 (T)	35 (T)	40 (T)
Maximum stress for T	217 (T)	256 (T)	295 (T)
Maximum stress for C	-513 (C)	-605 (C)	-696 (C)

Unit of stress in MPa. C: Compression, T: Tension.

TABLE VIII  
STRESSES AND J-INTEGRAL OF CIGS CELL WITH AN INITIAL CRACK AFTER COOLING DOWN TO ROOM TEMPERATURE FROM VARIOUS HOTSPOT TEMPERATURES (USING THE CELL WITH 400 °C ANNEALING AND 1% MAX BENDING)

Hotspot temperature	200 °C	300 °C	400 °C
ZnO layer stress (Avg)	-379 (C)	-447 (C)	-515 (C)
CdS layer stress (Avg)	-87 (C)	-102 (C)	-118 (C)
CIGS layer stress (Avg)	27 (T)	31 (T)	36 (T)
Maximum stress for T	1465 (T)	1726 (T)	1988 (T)
Maximum stress for C	-2007 (C)	-2365 (C)	-2724 (C)
J-integral (J/m <sup>2</sup> )	0.32	0.38	0.44

Unit of stress in MPa. C: Compression, T: Tension.

the energy release rate increases, which confirms that the probability of delamination between the CdS/CIGS layer increases as bending load and annealing temperature increase. However, to the best of authors' knowledge, the value of critical energy release rate at the CdS/CIGS interface is not known, so we are not able to determine whether actual delamination would occur or not. Finding the critical energy release rate of the CdS/CIGS interface would be the future work of our group.

### C. Hotspot Temperature Effect on Internal Stresses

Sometimes, rollable CIGS solar cells are unrolled and hung on camping tents or backpacks to charge small electronic devices. After charging the electronic devices for a while, people roll the solar cell again and store it inside a backpack. However, it is possible for the solar cell to experience a partial shading due to environmental conditions while charging. In that case, the solar cell would experience a hotspot temperature followed by returning to the environmental temperature. We calculated the internal stress of each layer of the CIGS after cooling down to room temperature from several hotspot temperatures: 200, 300, and 400 °C. Our simulated solar cell length is 10 μm, which is much smaller than the real size of partial shading of CIGS cell. So, the entire cell is treated as a hotspot region.

Table VII illustrates the stress of each active layer of CIGS cell without an initial crack after cooling down to room temperature from various hotspot temperatures (using the cell with previous 400 °C annealing and 1% max bending). It was found that the stress of each layer is higher when exposed to higher hotspot temperature.

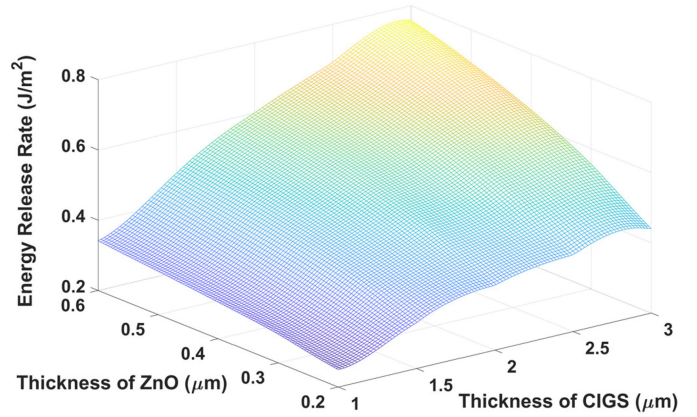


Fig. 6. Effect of the thickness of CIGS and ZnO on the energy release rate of CIGS solar cell with an initial crack: thickness of CdS is fixed to 0.05 μm.

Moreover, Table VIII shows the effect of hotspot temperature on the stresses and *J*-integral of CIGS cell with an initial crack. Again, the stress of each layer and *J*-integral increase as hotspot temperatures increase, which confirms the higher delamination probability with higher hotspot temperature.

It is possible to have phase or microstructure change if the CIGS cell goes through high temperatures. Those changes might be predicted using molecular dynamics or *ab initio* simulations. However, FEM simulation considering phase or microstructure change due to thermal treatment is beyond our scope, which can be future work of our group.

### D. Effect of Active Layer Thickness on Delamination

Fig. 6 illustrates the effect of the thickness of CIGS and ZnO on the energy release rate of CIGS cell with an initial crack when the thickness of CdS is fixed to 0.05 μm. For this simulation, we applied 400 °C annealing temperature and cooling to room temperature, bending with 1% maximum strain followed by 400 °C hotspot temperature. The energy release rate of 3 μm CIGS layer thickness is 1.8 times higher than that of 1 μm CIGS layer thickness when the thickness of ZnO layer is 0.2 μm, while 2.2 time higher when the thickness of the ZnO layer is 0.6 μm. Therefore, CIGS cell manufacturers can quantitatively relate the CIGS layer thickness with delamination probability for optimal design of the CIGS solar cell.

We also performed the same simulations with several CdS thicknesses ranging from 0.05 to 0.07 μm. From the simulation results, it was observed that the CIGS thickness is the most significant on the delamination of the CdS/CIGS interface compared with the thickness of ZnO and CdS. Variation of CdS thickness ranging between 0.05 and 0.07 μm minimally changed the energy release rate. However, the influence of ZnO thickness on the energy release rate is more significant than the thickness of CdS, but less significant than the thickness of CIGS.

### E. Delamination Length Effect on Electrical Performance

Fig. 7 shows the effect of delamination percentage of CdS/CIGS interface on the electrical performance of the CIGS

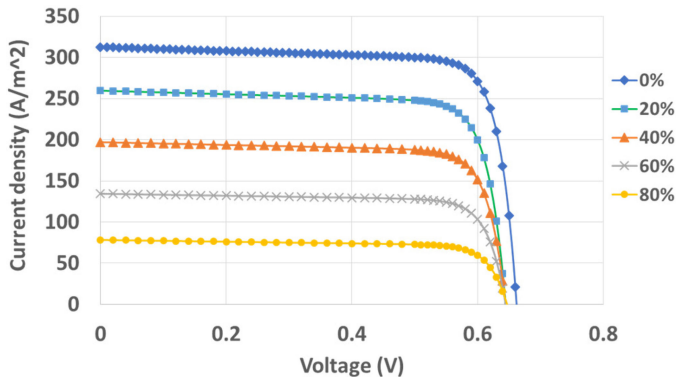


Fig. 7. Effect of delamination percentage of CdS/CIGS interface on the electrical performance of CIGS solar cell.

cell. As delamination length increases, short-circuit current density decreases significantly due to the loss of area of p-n junction. However, compared with the substantial decrease of the short-circuit current density, the loss of open-circuit voltage is negligible, which agrees with the experimental result of Lee *et al.* [3]. For example, as crack length increases from 0% to 80%,  $V_{oc}$  decreased from 0.66 to 0.64 V (3% decrease), while  $J_{sc}$  decreased from 313 to 78 A/m<sup>2</sup> (75% decrease).

#### IV. CONCLUSION

We investigated the effect of annealing temperature, bending loads, and hotspot temperature on the thermo-mechanical stress of each active layers as well as energy release rate ( $J$ -integral) through FEM analysis. We found that the average stress of each active layer decreases and maximum stress in the cell increases when interface crack is introduced between CdS/CIGS. With higher annealing and hotspot temperatures, thermal stresses and energy release rate in the cell are higher when the CIGS cell is cooled down to room temperature. For the cells without initial crack, maximum tensile stress occurs at the CdS/CIGS interface while maximum compressive stress occurs at the CdS/ZnO interface. For the cells with initial crack, maximum tensile stress takes place at the upper region of crack tip, while maximum compressive stress takes place at the lower region of crack tip. It is also found that lowering the annealing temperature can reduce the stresses in the cells and lowering the CIGS thickness can reduce the delamination probability of the CdS/CIGS interface.

Finally, we investigated the effect of crack length of the CdS/CIGS interface on the electrical performance of CIGS solar cells through FEM simulation. It was found that short-circuit current density decreases as the crack size increases. However, open-circuit voltage is minimally influenced by the crack size, which agrees with the experimental result of the published literature.

#### REFERENCES

- [1] D. J. L. Brémaud, "Investigation and development of CIGS solar cells on flexible substrates and with alternative electrical back contacts," *Ph.D. dissertation*, ETH, Zurich, Switzerland, 2009.
- [2] S. Y. Park *et al.*, "Investigation of ZnO/CdS/CuInxGa<sub>1-x</sub>Se<sub>2</sub> interface reaction by using hot-stage TEM," *Current Appl. Phys.*, vol. 10, no. 3, pp. S399–S401, May 2010.

- [3] S. M. Lee, D. H. Yeon, B. C. Mohanty, and Y. S. Cho, "Tensile stress-dependent fracture behavior and its influences on photovoltaic characteristics in flexible PbS/CdS thin-film solar cells," *ACS Appl. Mater. Interfaces*, vol. 7, no. 8, pp. 4573–4578, Mar. 2015.
- [4] K. A. Sierros *et al.*, "Mechanical properties of ZnO thin films deposited on polyester substrates used in flexible device applications," *Thin Solid Films*, vol. 519, no. 1, pp. 325–330, Oct. 2010.
- [5] H. X. Mei, Y. Y. Pang, S. H. Im, and R. Huang, "Fracture, delamination, and buckling of elastic thin films on compliant substrates," in *Proc. 11th Intersoc. Conf. Thermal Thermomech. Phenomena Electron. Syst.*, Orlando, FL, USA, 2008, pp. 762–769.
- [6] H. Chai and J. Fox, "On delamination growth from channel cracks in thin-film coatings," *Int. J. Solids Struct.*, vol. 49, no. 22, pp. 3142–3147, Nov. 2012.
- [7] J. E. Lee *et al.*, "Investigation of damage caused by partial shading of CuInxGa<sub>1-x</sub>Se<sub>2</sub> photovoltaic modules with bypass diodes," *Prog. Photovolt.*, vol. 24, no. 8, pp. 1035–1043, Aug. 2016.
- [8] M. Nardone, S. Dahal, and J. M. Waddle, "Shading-induced failure in thin-film photovoltaic modules: Electrothermal simulation with nonuniformities," *Sol. Energy*, vol. 139, pp. 381–388, Dec. 2016.
- [9] S. Dongaonkar, C. Deline, and M. A. Alam, "Performance and reliability implications of two-dimensional shading in monolithic thin-film photovoltaic modules," *IEEE J. Photovolt.*, vol. 3, no. 4, pp. 1367–1375, Oct. 2013.
- [10] Y. C. Lin *et al.*, "Residual stress in CIGS thin film solar cells on polyimide: Simulation and experiments," *J. Mater. Sci., Mater. Electron.*, vol. 25, no. 1, pp. 461–465, Jan. 2014.
- [11] A. Hazarika *et al.*, "STM verification of the reduction of the Young's modulus of CdS nanoparticles at smaller sizes," *Surf. Sci.*, vol. 630, pp. 89–95, Dec. 2014.
- [12] A. JemmyCinthia, G. Sudhapriyanga, R. Rajeswarapalanichamy, and M. Santhosh, "Structural, electronic and elastic properties of ZnO and CdO: A first-principles study," in *Proc. Int. Conf. Adv. Manuf. Mater. Eng.*, 2014, vol. 5, pp. 1034–1042.
- [13] M. Gloeckler, A. L. Fahrenbruch, and J. R. Sites, "Numerical modeling of CIGS and dTe solar cells: Setting the baseline," in *Proc. 3rd World Conf. Photovolt. Energy Convers.*, 2003, pp. 491–494.
- [14] R. J. Sanford, *Principle of Fracture Mechanics*. Englewood Cliffs, NJ, USA: Prentice-Hall, 2003.
- [15] M. Gloeckler, *Device Physics of Cu(In,Ga)Se<sub>2</sub> Thin-Film Solar Cells*. Fort Collins, CO, USA: Colorado State Univ., 2005.
- [16] H. Kim, M. T. Tofail, and C. John, "The effect of interface cracks on the electrical performance of solar cells," *JOM*, vol. 70, no. 4, pp. 473–478, Apr. 2018.
- [17] R. Hibbeler, *Mechanics of Materials*. Englewood Cliffs, NJ, USA: Prentice-Hall, 2004.



**Hansung Kim** (M'17) received the M.S. degree in dynamic battery modeling of hybrid electric vehicles and the Ph.D. degree in multiscale modeling of micro- and nanoscale thin films from The Ohio State University, Columbus, OH, USA, in 2002 and 2008, respectively.

From 2008 to 2012, he was a Postdoctoral Researcher with Purdue University, West Lafayette, IN, USA, and Northwestern University, Evanston, IL, USA. He is currently an Assistant Professor with the Department of Mechanical and Civil Engineering, Purdue University Northwest, Hammond, IN, USA. His research interests include multiscale modeling and characterization of advanced nano/bio/energy systems and materials. The scope of his multiscale modeling and characterization ranges from atomistic to macro scales utilizing both theoretical and experimental studies.

Dr. Kim is a member of ASME and TMS.



**Da Xu** received the B.S. degree in mechanical engineering from Southwest University of Science and Technology, Mianyang, China, in 2012. He is currently working toward the M.S. degree in mechanical engineering in Purdue University Northwest, Hammond, IN, USA.

His research interests include modeling of solar cells.



**Yaqiong Wu** received the M.S. degree in mechanical engineering from Purdue University Northwest, Hammond, IN, USA, in 2018.

She is working on solar cell research during her study time. Her research interests include finite element analysis.



**Ciby John** received the M.S. degree from Purdue University Northwest, Hammond, IN, USA, in 2018.

His research interests include finite element modeling for predicting the effect of mechanical failure on semiconductor performance using multiphysics software.